Observation of Fe(V)=O using Temperature Variable Mass Spectrometry and its Enzyme-like C-H and C=C Oxidation Reactions

Irene Prat[a], Jennifer S. Mathieson[b], Mireia Güell,[c] Xavi Ribas[a], Josep M. Luis,[c] Leroy Cronin[b]*, Miquel Costas[a]*

[a]*Department de Química, Universitat de Girona, Campus de Montilivi, Girona, 17071, Spain*

[b]*WestCHEM, School of Chemistry, The University of Glasgow, Glasgow, G12 8QQ, UK*

[c]*Institut de Química Computacional, Universitat de Girona, Campus de Montilivi, Girona, 17071, Spain*

*To whom correspondence should be addressed. Email: miquel.costas@udg.edu and L.Cronin@chem.gla.ac.uk

Oxo transfer chemistry mediated by iron underpins many biological processes and today is emerging as synthetically very important for the catalytic oxidation of conventionally hard to activate C-H and C=C moieties.[1-6] Despite the vast amount of research in this area, the identity of the reactive species under catalytic conditions has not been observed, although the Fe(V)=O species has been postulated as being this species.[4] Herein, using temperature variable mass spectrometry, we were able to observe the Fe(V)=O within the synthetic $[Fe^{V}(O)(OH)(^{Me,H}Pytacn)]^{+}$ (^{Me,H}Pytacn = 1-(2'-pyridylmethyl)-4,7-dimethyl-1,4,7-triazacyclononane) complex at -40 ºC and its reaction with an olefin. We were also able to follow oxygen atom transfer from H_2O_2 / H_2O through Fe(V)=O to the products with isotopic labelling, as well as probe the reactivity as a function of temperature. This is the first ever implementation of temperature variable mass spectrometry to investigate reactive intermediates.

When it comes to small molecule activation processes, iron is the element of choice, selected by nature in order to perform a number of chemically challenging oxidative processes with high precision and reaction rates. Iron-based enzymes such as Cytochrome P450[1] and Rieske

dioxygenases,[7] among others, use O_2 to catalyze highly selective C-H and C=C oxidation reactions, as key steps in the metabolic synthesis of metabolites, and xenobiotic degradation, among other crucial functions. At the heart of these transformations, it is proposed that the catalytic iron centre forms a highly oxidising ferryl species (Scheme 1).[8] In P450 the ferryl species (formally Fe(V)=O), is best described as a oxo-Fe^{IV}-porphyryl radical cation,[1] but in the case of the Rieske dioxygenases family of enzymes, which lack the red-ox non innocent porphyrin ligand, an oxo-iron(V) species has been postulated as being the reactive species.[9,10] The observation of these highly reactive intermediates remains a formidable challenge that has been recently solved for P450,[11] but so far it has not been accomplished in a non-heme enzyme.[12,13]

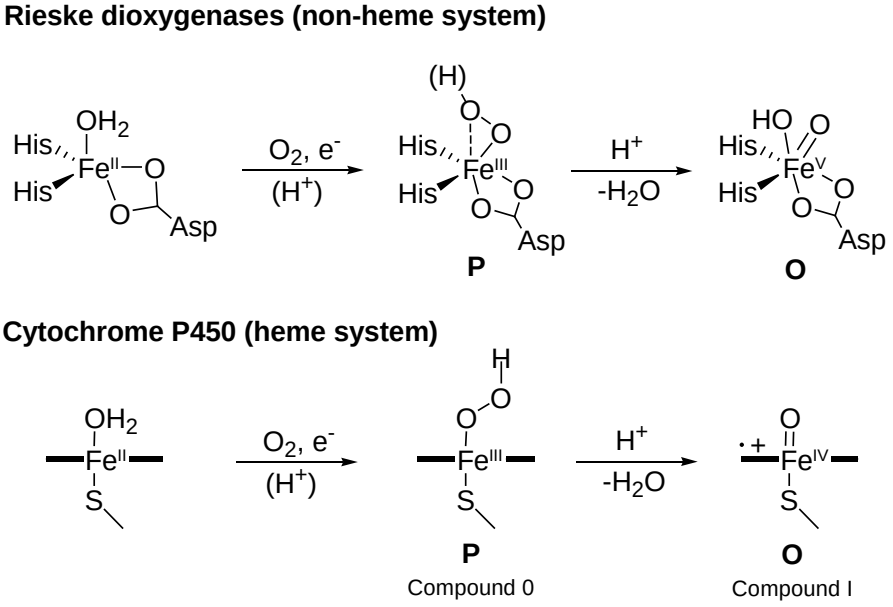

Scheme 1. Mechanistic proposals for the formation of formally oxo-iron(V) species in Rieske Dioxygenases and P450.

Functional models of non-heme iron dependent oxygenases are the focus of current major research efforts due to the major challenges in modern synthetic chemistry that selective and environmentally benign C-H hydroxylation and olefin *cis*-dihydroxylation reactions represent, with the aim of such studies being to gain an intimate understanding of the processes underpinning the

enzymatic reactions.[4-6,14] Mechanistic studies of naphthalene 1,2-dioxygenase,[13,15] a member of the Rieske dioxygenases family, and of model compounds[16-21] point strongly towards the involvement of a highly electrophilic oxo-iron(V) species, yet direct evidence *under catalytic conditions* is lacking.[22,23] In this respect the development of temperature variable mass spectrometry (TV-MS) could be used as a very powerful technique to allow the study of highly reactive intermediate species at very low reagent concentrations, without the need of large product accumulation required for most spectroscopic techniques. TV-MS could also be used to follow the emergence of the reactive species under much colder conditions normally used in electrospray mass spectrometric experiments, thus minimizing bimolecular decomposition pathways commonly associated with highly-reactive species. Therefore we envisaged that the observation of reactive species may not only be possible by using low temperature mass spectrometry[24-29], but we also postulated that varying the temperature of the electrospray source during the experiment under catalytic conditions may also give further insight and evidence of the identity of the reactive intermediate.

Cryospray mass spectrometry (low temperature mass spectrometry) has not been used before to follow reactive intermediates, and herein we present a new technique that uses cryrospray technology to allow temperature variable mass spectrometry (TV-MS). This technique allowed the temperature controlled trapping and characterization of a Fe(V)=O species which acts as a functional model of Rieske dioxygenases. Isotopic labelling studies have been used to provide unambiguous chemical description of these species, and have demonstrated atom transfer from the reagent, via the Fe-complex, into the product i.e. the *cis*-dihydroxylation of an olefin. The data presented in this work allowed us to elucidate the nature of the iron-based species responsible for performing alkane hydroxylation and olefin *cis*-dihydroxylation in synthetic and enzymatic systems.

Results and Discussion

The non-heme iron complex [Fe(CF_3SO_3)$_2$(^{Me,H}Pytacn)] (**1**) (Scheme 2) catalyzes the hydroxylation of alkanes and *cis*-dihydroxylation of alkenes using H_2O_2 as oxidant, and thus it constitutes a functional model of the Rieske dioxygenases family of enzymes.[19,20] The hydroxylation of *cis*-1,2-dimethylcyclohexane is stereospecific and affords a racemic mixture of *1R,2R-trans*-dimethylcyclohexanol and *1S,2S-trans*-dimethylcyclohexanol (Scheme 2). Likewise, oxidation of *cis*-2-heptene by **1** is *syn*-stereospecific and affords a 2:1 racemic mixture of 95% *erythro*-heptane-2,3-diol and *2*-butyl-3-methyloxirane (97% *cis*). When the catalytic reactions are performed in the presence of $H_2{}^{18}O$, the oxidized products exhibit a correspondingly large content of ^{18}O (Scheme 2); alcohols *1R,2R-trans*-dimethylcyclohexanol and *1S,2S-trans*-dimethylcyclohexanol are 76±3% ^{18}O-labeled, while *erythro*-diol is 84±3% $^{16}O^{18}O$ labelled, that is one of the two oxygen atoms was derived from H_2O. The complementary experiment using $H_2{}^{18}O_2$ as oxidant showed that the second oxygen atom was derived from the peroxide. The isotopic labelling experiments, in combination with DFT computational methods allowed us to confidently propose that a $Fe^V(O)(OH)$ species is responsible for the C-H and C=C oxidation events.[19,20] Such a mechanistic scenario has been previously proposed for related non-heme iron catalysts,[16-18] but no direct spectroscopic evidence of the putative high-valent species, with the benefit of isotopic labelling, has been obtained so far.[24]

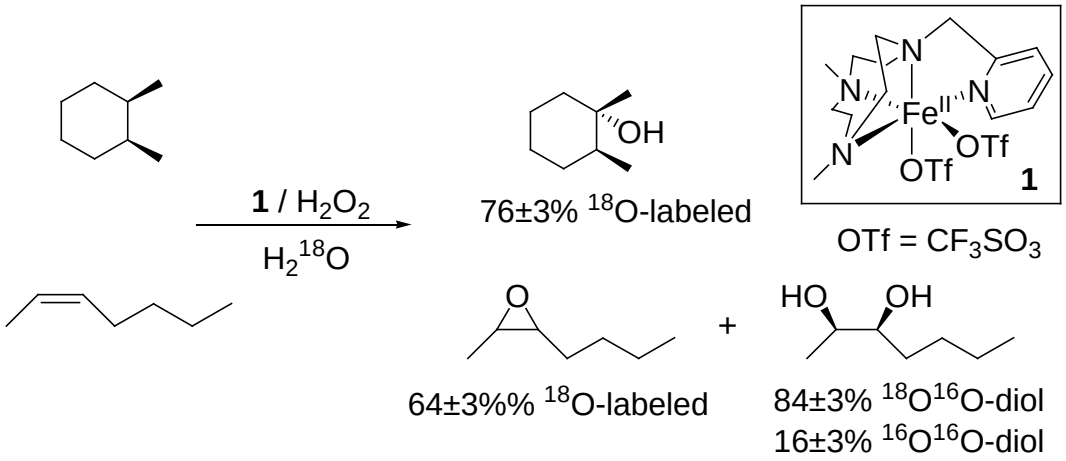

Scheme 2. Stereospecific hydroxylation of *cis*-1,2-dimethylcyclohexane (1000 equiv.) (top) and epoxidation and *cis*-dihydroxylation of 2-heptene (1000 equiv.) (bottom) with H_2O_2 (10 equiv.), catalyzed by **1**, in the presence of $H_2{}^{18}O$ (1000 equiv.).

Monitoring of the reaction of **1** with H_2O_2 by UV-vis spectroscopy in a range of temperatures from room temperature (RT) to -40 ºC, did not lead to accumulation / observation of any intermediate species. Therefore the reaction was explored at between room temperature and -40 ºC by using temperature variable (cryospray) mass spectrometry (TV-MS) with the aim of observing the elusive reaction intermediates that could be present at low, presumably steady-state concentrations. CSI-MS analysis of the reaction of **1** with H_2O_2 (100 equiv) between 20 ºC and -40 ºC showed the growth of a prominent peak at m/z = 470.1 that was assigned to $\{[Fe^{III}(OH)(^{Me,H}Pytacn)](CF_3SO_3)\}^+$, **2**, and a second, less intense peak at m/z = 486.1 = M, which could be formulated as $\{[Fe^{III}(OOH)(^{Me,H}Pytacn)](CF_3SO_3)\}^+$, **3P**, or $\{[Fe^{V}(O)(OH)(^{Me,H}Pytacn)](CF_3SO_3)\}^+$, **3O** on the basis of its m/z and isotopic distribution ratio. This second peak was not observed when reactions were performed at room temperature, and it rapidly disappeared as the temperature was raised from -40 ºC to room temperature. This directly implied that **3** was the metastable reaction intermediate (Figure 1).

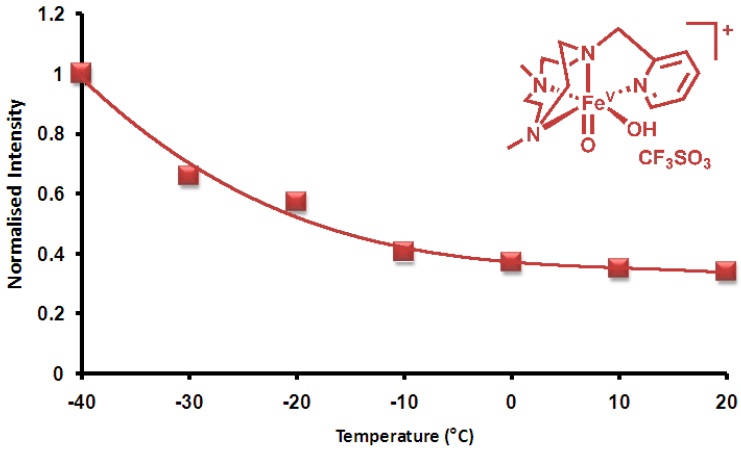

Figure 1. Graph showing the decomposition of **3P**/**3O** species (486 *m/z*) when the temperature is increased from -40 °C to 20 °C using the TV-MS technique.

In order to distinguish between the two possible formulations for **3**, isotopic labelling experiments were conducted. Because of consistency with our catalytic reactions experiments, and also the experimental limitations of the isotopically labelled reagents ($H_2{}^{18}O_2$ is a 2% w:w solution in water), we studied 1) the reaction of **1** with H_2O_2 (10 equiv) in the presence of $H_2{}^{18}O$ (1000 equiv), 2) the complementary experiment involving the reaction of **1** with $H_2{}^{18}O_2$ (16 equiv.) in the presence of H_2O (1000 equiv) and 3) the reaction of **1** with $H_2{}^{18}O_2$ (10 equiv.) in the presence of $H_2{}^{18}O$ (1000 equiv). However, because our $H_2{}^{18}O_2$ solutions are 2% in $H_2{}^{16}O$, over 300 equiv of $H_2{}^{16}O$ were also present in solution in this experiment.

Most remarkably, the spectrum of the reaction of **1** with $H_2{}^{16}O_2$ in the presence of $H_2{}^{18}O$ showed a new cluster peak assigned to **3**, which was now displaced by two m/z units and centred at m/z = 488.1 = M+2. (Figure **2B**). The complementary experiment using $H_2{}^{18}O_2$ and $H_2{}^{16}O$, confirmed our initial formulation,[19,20] and showed a peak centred at m/z = 488.1 = M+2 (Figure **2C**). Finally, **3O** was generated by using $H_2{}^{18}O_2$ (10 equiv.) in the presence of $H_2{}^{18}O$ (1000 equiv.), (Figure **2D**). In this case, the peak at m/z = 488.1 = M+2 continue to be the major species, but a peak at m/z = 490.1 = M+4 appeared as the second most intense component of the spectrum. The large intensity of the M+2 peaks is partially explained because the sample contained a large amount

of $H_2{}^{16}O$ that came from the $H_2{}^{18}O_2$ reagent (2% solution in $H_2{}^{16}O$). In addition, the large amount of water present in this experiment decreased the intensity and stability of the ion peaks associated to **3O**[30] (see supporting information S4 for the full explanation). Since the peroxide type species does not exchange their oxygen atoms with water,[28] the isotopic labelling observations appeared incompatible with **3P**. Instead, the MS isotopic labelling experiments provided strong indication that **3** must be described as $\{[Fe^{V}(O)(OH)(^{Me,H}Pytacn)](CF_3SO_3)\}^{+}$, where a single oxygen atom was derived from H_2O_2, and a second oxygen atom was derived from H_2O, presumably *via* a water assisted heterolytic O-O breakage in a hydroperoxide $\{[Fe^{III}(OOH)(OH_2)(^{Me,H}Pytacn)](CF_3SO_3)\}^{+}$, **3P·H₂O** species (Figure 2, top).[32] Isotopic labelling experiments showed that optimum simulation of the spectra shown in figures **2B** and **2C** required ~10% contribution of species with m/z = M+4. These species were assigned to $\{[Fe^{III}(OH)(^{18}OH_2)(^{Me,H}Pytacn)](CF_3SO_3)\}^{+}$ and $\{[Fe^{III}(^{18}OH)(OH_2)(^{Me,H}Pytacn)](CF_3SO_3)\}^{+}$, corresponding to the acqua-ligated form of **2**. Although the MS data does not provide direct indication of the oxidation state of the iron site, we concluded that Fe^{V} was the most plausible oxidation state because of the redox innocence of all the ligands, with this is also being consistent with DFT analysis of this species.[19,20]

Having established good evidence for the identity of **3O**, we sought to demonstrate its reactivity with respect to an intermolecular oxidation reaction, as this would provide further proof that **3O** is reactive as predicted by our mass spectrometric assignment. To do this, we chose a reaction with an olefin because we envisioned that should **3O** perform a olefin *cis*-dihydroxylation reaction; i.e. it would form a kinetically stable iron-(hydrogen)glycolate species (Figure 3, top). In such case, the use of ^{18}O labels were also used as a powerful tool to demonstrate that the transformation was indeed mediated by the reactive Fe(V)=O species assigned to the identity of **3O**.

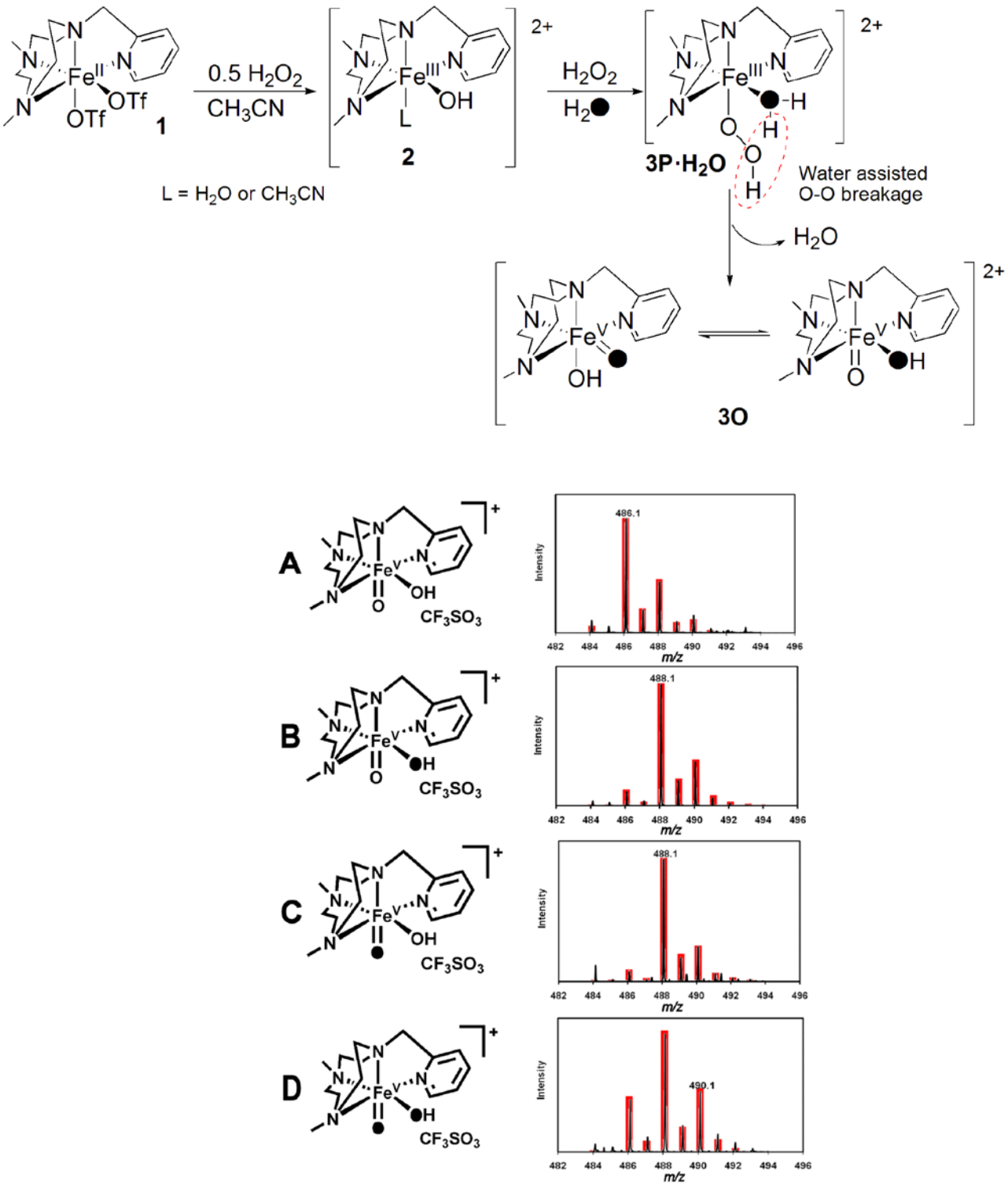

Figure 2. (Top); Mechanistic diagram for the formation of the oxo-iron(V) species **3O**, via a water assisted heterolytic cleavage of the O-O bond in **3P·H2O.** (Bottom)**;** CSI-MS spectra in acetonitrile solution at -40 ºC. Red-bars correspond to the simulated data, (see supporting info for the full analysis of the isotopic envelope) while black lines correspond to the experimental data. A) **3O** generated with $H_2{}^{16}O_2$ (10 equiv.) in the presence of $H_2{}^{16}O$ (1000 equiv). B) **3Oa, 3O** generated

with $H_2{}^{16}O_2$ (10 equiv.) in the presence of $H_2{}^{18}O$ (1000 equiv). C) **3Ob, 3O** generated with $H_2{}^{18}O_2$ (16 equiv.) in the presence of $H_2{}^{16}O$ (1000 equiv). D) **3Oc, 3O** generated with $H_2{}^{18}O_2$ (10 equiv.) in the presence of $H_2{}^{18}O$ (1000 equiv). (All calculated peaks fit the statistical treatment of experimental error).

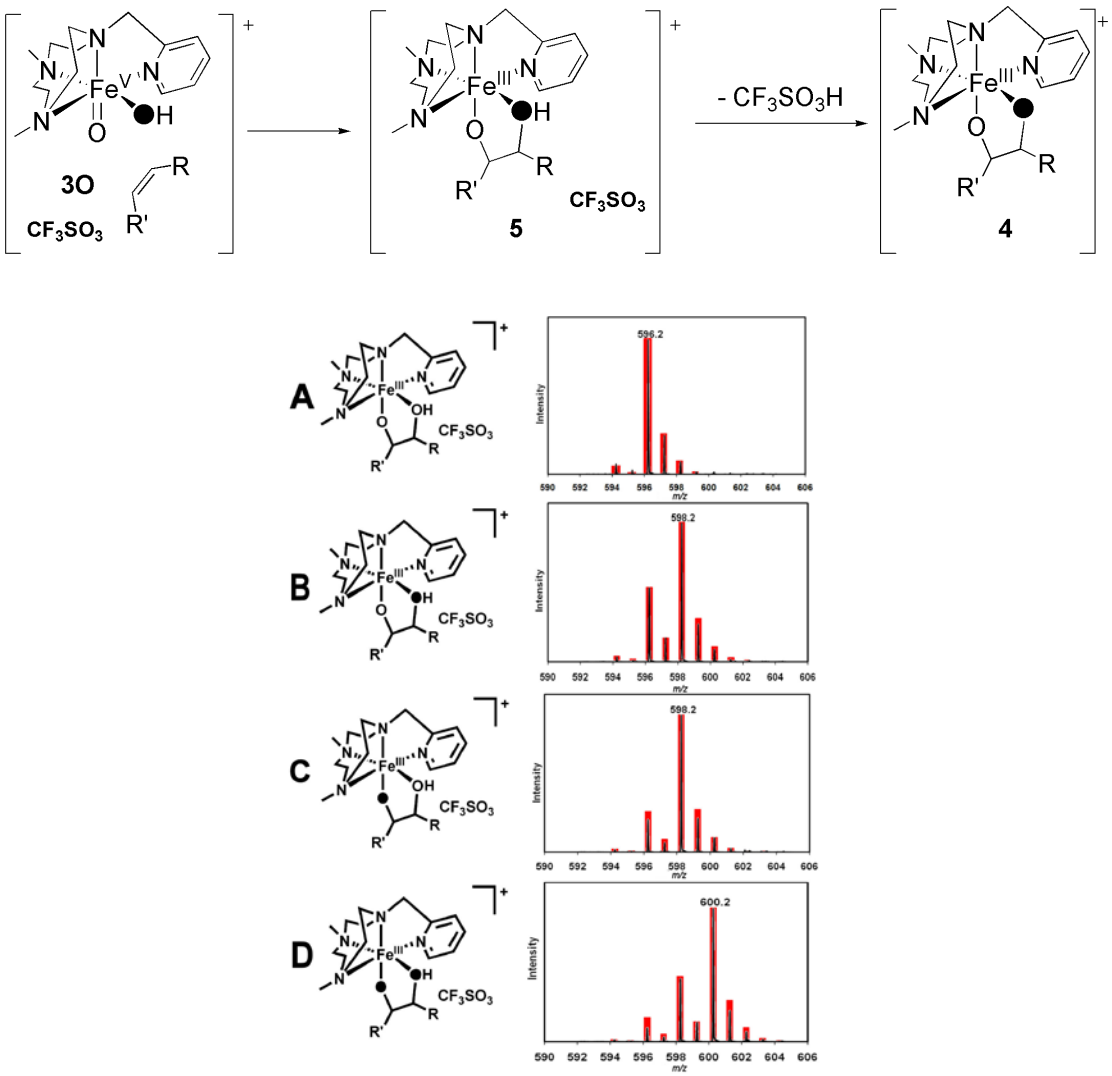

Figure 3. (Top); Mechanistic diagram for the reaction between the oxo-iron(V) species **3P** with an olefin to form hydrogenglycolate species **5**, and glycolate species **4**. (Bottom); CSI-MS spectra in acetonitrile solution at -40 ºC. Red-bars correspond to the simulation (See supporting info for the full analysis of the isotopic envelope), while black lines correspond to the experimental data. A) **5** formed by reaction of cyclooctene (100 equiv.) with **3O** (generated with $H_2{}^{16}O_2$ (3 equiv.) in the presence of $H_2{}^{16}O$ (1000 equiv)). B) **5a**, **5** formed by reaction of cyclooctene (100 equiv.) with **3O** (generated with $H_2{}^{16}O_2$ (3 equiv.) in the presence of $H_2{}^{18}O$ (1000 equiv). C) **5b, 5** formed by

reacting cyclooctene (100 equiv.) with **3O** (generated with $H_2{}^{18}O_2$ (3 equiv.) in the presence of $H_2{}^{16}O$ (1000 equiv)). D) **5c**, **5** formed by reacting cyclooctene (100 equiv.) with **3O** (generated with $H_2{}^{18}O_2$ (3 equiv.) in the presence of $H_2{}^{18}O$ (1000 equiv)). (All calculated peaks fit the statistical treatment of experimental error).

To this end, **3O** was generated and reacted with cyclooctene (100 equiv.) at -40 ºC. MS analysis of the reaction indicated that the cluster peak assigned to **3** had disappeared, and new peaks at m/z = 446.2 and m/z = 596.2 (Figure 3A) had emerged. The isotopic pattern of these ions could be successfully simulated as the complexed glycolate species $[Fe^{III}(C_8H_{14}O_2)(^{Me,H}Pytacn)]^+$, **4** and the complexed hydrogenglycolate species $\{[Fe^{III}(C_8H_{14}(O)(OH))(^{Me,H}Pytacn)](CF_3SO_3)\}^+$, **5** (**4**+$H^+$+$CF_3SO_3$), resulting from a *cis*-dihydroxylation reaction of **3** with cyclooctene. (See supporting information for the spectrum of dihydroxylation of 1-octene and cyclohexene).

GC and GC-MS analysis at the end of the low temperature reaction with cyclooctene showed that the expected epoxides (0.9 TN) and diols (1.0 TN) were formed. M/z and isotopic patterns assigned to **4** and **5** could also support alternative epoxide-bound formulations $[Fe^{III}(O)(C_8H_{14}O)(^{Me,H}Pytacn)]^+$, for **4** and $\{[Fe^{III}(OH)(C_8H_{14}(O))(^{Me,H}Pytacn)](CF_3SO_3)\}^+$, for **5**. However, epoxides are well-known to be very poor ligands with putative epoxide bound species dissociating very fast, thus being kinetically unstable. Ion peaks corresponding to **4** and **5** remained stable over time, and did not show oxygen exchange with water molecules from the reaction mixture. Also, the lack of water exchange that hydroxide and oxide ligands in thermally stable Fe(III) complexes will engage in and the stability of the ion peaks associated to **4** and **5** points towards no observation of epoxide bound formulations. Therefore, we can conclude that epoxide bound species could not be detected in the spectra.

Further evidence that **3O** was the reactive intermediate came from isotopic labelling experiments. **3O** (**3Oa**) was generated with $H_2{}^{16}O_2$ in the presence of $H_2{}^{18}O$ (1000 equiv) and reacted with cyclooctene (100 equiv.). In this case (Figure 3B), the cluster ion associated to **5** (**5a**) was displaced by 2 mass units. Likewise, when **3O** (**3Ob**) was generated with $H_2{}^{18}O_2$ in the

presence of $H_2{}^{16}O$ (1000 equiv), and then reacted with cyclooctene (100 equiv.), the spectrum (Figure 3C) shows again the formation of cluster ions at m/z = 448.2 and m/z = 598.2 assigned to **4b** and **5b**, respectively. Analogous results were obtained when 1-octene and cyclohexene were chosen as substrates (see supporting information). These observations led us to conclude that **3O** constitutes a reaction intermediate that precedes formation of **4** and **5** upon reaction with an olefin.

We have previously described on the basis of DFT computations that water assisted transformation of **3P** into **3O** is thermoneutral and has a small ($\Delta G^{\neq}$ = 20 kcal·mol^{-1}) activation barrier,[19-20] in good agreement with literature values for related non-heme iron complexes.[32-33] For comparison, homolytic breakage of the O-O bond in the Fenton intermediate $[(H_2O)_5Fe^{III}OOH]^{2+}$ is computed to have a comparable barrier of 21 kcal·mol^{-1}.[34] In order to substantiate the proposal that the $Fe^{V}(O)(OH)$ species is indeed the executor of the *cis*-dihydroxylation event, the reaction of **3O** with 2-butene, as a model substrate was also computed by DFT methods.[35] A summary of DFT results are illustrated in Fig. 4. The dihydroxylation is strongly exergonic, being **5** 60.96 kcal·mol^{-1} more stable than **3O**. In addition, the reaction proceeds with very small energy barriers. The ground state of **3O** is S = 3/2, and it is well separated in energy by 11.50 Kcal·mol^{-1} with respect to the first excited state (S= 1/2). The attack of the hydroxo ligand over the olefin leads to the formation of the first C1-O1 bond, forming intermediate **I**, with a small barrier of $\Delta G^{\neq}$ = 3.32 kcal·mol^{-1}. **I** then evolves via attack of the oxo ligand over C2, without an energy barrier and leads to the direct formation of the gycolate species **5**. We notice that the concerted, yet unsymmetric nature of the *cis*-dihydroxylation event derived from our calculations bears strong resemblance to the analysis recently described by Che et al for the *cis*-dihydroxylation reaction mediated by a non-heme iron complex, upon reaction with Oxone.[24] On the other hand, on the basis of product analyses and DFT calculations, two recent studies have proposed that $Fe^{IV}(OH)_2$ species could be responsible for *cis*-dihydroxylation reactions in selected iron catalysts.[36,37] These catalysts exhibit different reactivity patterns with respect to the [Fe(^{Me,H}Pytacn)] system described in this work. In the former cases,

isotopic analysis shows that *cis*-dihydroxylation preferentially takes place via insertion of two oxygen atoms from a single H_2O_2 molecule.

Further evidence for a different mechanistic scenario was provided by the observation that $[Fe^{IV}(O)(OH_2)(^{Me,H}Pytacn)]^{2+}$ does not mediate the *cis*-dihydroxylation of olefins. This complex was recently prepared and spectroscopically characterized by us,[38] and computational analyses indicate that a $[Fe^{IV}(OH)_2(^{Me,H}Pytacn)]^{2+}$ intermediate is involved in its water exchange reactions.

In conclusion, the mechanisms underlying *cis*-dihydroxylation reactions mediated by $[Fe(OTf)_2(^{Me,H}Pytacn)]$ are likely to be fundamentally distinct from these operating through a Fe^{II}/Fe^{IV} cycle.

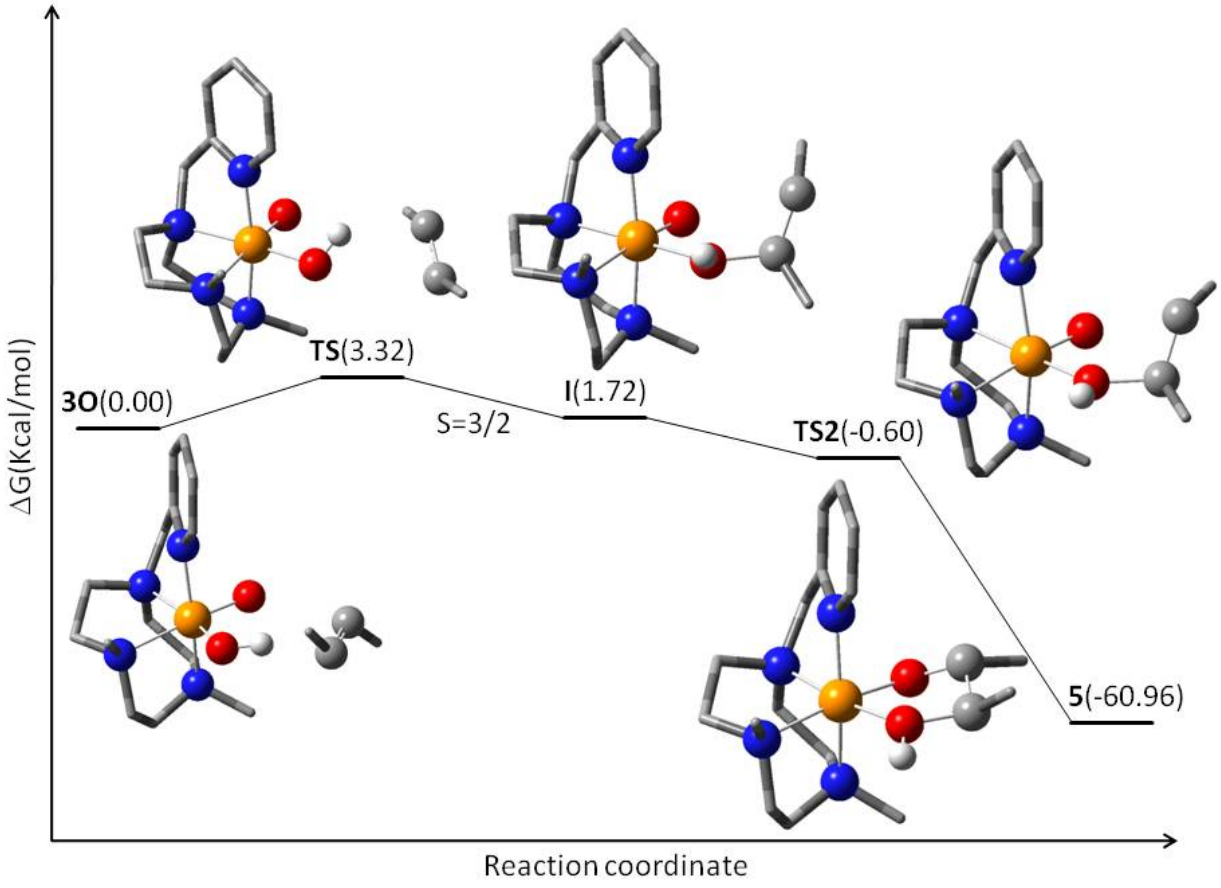

Figure 4. Mechanistic diagram for the DFT analysis of the reaction between the oxo-iron(V) species **3O** with 2-butene to form hydrogenglycolate species **5** (See supporting info for full details on the computational methods).

Conclusions

Previous computational and product analysis experiments in catalytic C-H hydroxylation and C=C *cis*-dihydroxylation reactions mediated by non-heme iron catalysts have previously predicted **$Fe^{V}(O)(OH)$** species as the real oxidant that executes very fast stereospecific C-H and C=C oxidation reactions.[16-20,32,33] With this work we have presented the development and first ever application of TV-MS to the investigation of the reaction between the non-heme iron catalyst **1** with H_2O_2 between + 20 and -40 ºC, which has led to the first experimental evidence for the identification of a metastable intermediate that could be formulated as $\{[Fe^{V}(O)(OH)(^{Me,H}Pytacn)](CF_3SO_3)\}^{+}$ **3O** on the basis of isotopic labelling experiments. Such experiments provide experimental evidence that **3O** contains an O atom that comes from H_2O_2 and a second O atom that originates from water, which in turn constitutes strong evidence for the assistance of a water-assisted path towards its generation (however direct kinetic proof is not yet available and will be the subject of further studies). Despite this limitation, isotopic labelling experiments demonstrated that **3O** precedes the *cis*-dihydroxylation reaction of olefins. This study provides the first experimental evidence, corroborated by a full DFT analysis, and isotopic labelling characterization for such a powerful oxidant, *under conditions relevant to catalysis*. Thus, results disclosed in this work provide new fundamental framework for understanding the nature of the iron-based species responsible for performing alkane hydroxylation and olefin *cis*-dihydroxylation in synthetic and enzymatic systems, as well as showing the potential of temperature variable mass spectrometry (TV-MS) in the investigation of reactive intermediates.

Methods

A Bruker microTOFQ Spectrometer with a cryospray attachment was used for ESI-MS and TV-MS. Samples were diluted to a maximum concentration of $5x10^{-5}$ M in acetonitrile and samples were injected at a rate of 180 μL per hour.

Procedure for Temperature controlled mass spectrometry. [Fe(^{Me,H}Pytacn)(CF_3SO_3)$_2$] (**1**) (0.5 mg, 8 x 10^{-4} mmols) was dissolved in MeCN (~ 7 ml) and the solution cooled to 4 ºC. A solution of H_2O_2 (10 mM in 10 ml MeCN) was made up and also cooled to 4 ºC. The solution of **1** (300 µl) was added to a vial that was cooled in a dry ice/MeCN bath and H_2O (15 µl) added. To this stirring solution H_2O_2 (300 µl, 3 x 10^{-3} mmols) was added (i.e. so the reaction mixture was injected at a lower temperature than -40 ºC) and the solution injected directly into the mass spectrometer (CSI-MS -40ºC). The spectrum was collected as a function of temperature, and the temperature variation of the cryospray source -40 to being around 20 ºC taking 15 minutes.

[Fe(^{Me,H}Pytacn)(CF_3SO_3)$_2$] (1). Synthesis was carried out using a reported procedure.[19] MS (CSI-MS -40ºC) *m/z* 453.1

{[Fe^{III}(OH)(^{Me,H}Pytacn)](CF_3SO_3)}$^+$ (2), {[Fe^{III}(OOH)(^{Me,H}Pytacn)](CF_3SO_3)}$^+$ (3P), **{[Fe^{V}(O)(OH)(^{Me,H}Pytacn)](CF_3SO_3)}$^+$ (3O)** [Fe(^{Me,H}Pytacn)(CF_3SO_3)$_2$] (**1**) (0.5 mg, 8 x 10^{-4} mmols) was dissolved in MeCN (~ 7 ml) and the solution cooled to 4 ºC. A solution of H_2O_2 (10 mM in 10 ml MeCN) was made up and also cooled to 4 ºC. The solution of **1** (300 µl) was added to a vial that was cooled in a dry ice/MeCN bath and H_2O (15 µl, 0.83 mmols) added. To this stirring solution H_2O_2 (300 µl, 3 x 10^{-3} mmols) was added and the solution injected directly into the mass spectrometer (CSI-MS -40ºC). The spectrum was collected immediately for 2 minutes. MS (CSI-MS) *m/z* 470.1 **(2)**, 486.1 **(3P, 3O).**

Procedure for isotopic labelled mass spectrometry.

{[Fe^{V}(O)(^{18}OH)(^{Me,H}Pytacn)](CF_3SO_3)}$^+$ (3Oa). [Fe(^{Me,H}Pytacn)(CF_3SO_3)$_2$] (**1**) (0.5 mg, 8 x 10^{-4} mmols) was dissolved in MeCN (~ 7 ml) and the solution cooled to 4 ºC. A solution of H_2O_2 (10 mM in 10 ml MeCN) was made up and also cooled to 4 ºC. A solution of H_2O_2 (650 mM in 10 ml MeCN) was made up and also cooled to 4 ºC. The solution of **1** (300 µl) was added to a vial that

was cooled in a dry ice/MeCN bath and $H_2{}^{18}O$ (15 µl, 0.83 mmols) added. To this stirring solution H_2O_2 (300 µl, 3 x 10^{-3} mmols) was added and the solution injected directly into the mass spectrometer (CSI-MS -40ºC). The spectrum was collected immediately for 2 minutes. MS (CSI-MS) *m/z* 488.1 **(3Oa).**

{[Fe^{V}(^{18}O)(OH)(^{Me,H}Pytacn)](CF$_3$SO$_3$)}$^+$ (3Ob). [Fe(^{Me,H}Pytacn)(CF$_3$SO$_3$)$_2$] (**1**) (0.5 mg, 8 x 10^{-4} mmols) was dissolved in MeCN (~ 7 ml) and the solution cooled to 4 ºC. A solution of $H_2{}^{18}O_2$ (10 mM in 10 ml MeCN) was made up and also cooled to 4 ºC. The solution of **1** (300 µl) was added to a vial that was cooled in a dry ice/MeCN bath and H_2O (15 µl, 0.83 mmols) added. To this stirring solution $H_2{}^{18}O_2$ (300 µl, 3 x 10^{-3} mmols) was added and the solution injected directly into the mass spectrometer (CSI-MS -40ºC). The spectrum was collected immediately for 2 minutes. MS (CSI-MS) *m/z* 488.1 **(3Ob).**

{[Fe^{V}(^{18}O)(^{18}OH)(^{Me,H}Pytacn)](CF$_3$SO$_3$)}$^+$ (3Oc). [Fe(^{Me,H}Pytacn)(CF$_3$SO$_3$)$_2$] (**1**) (0.5 mg, 8 x 10^{-4} mmols) was dissolved in MeCN (~ 7 ml) and the solution cooled to 4 ºC. A solution of $H_2{}^{18}O_2$ (10 mM in 10 ml MeCN) was made up and also cooled to 4 ºC. The solution of **1** (300 µl) was added to a vial that was cooled in a dry ice/MeCN bath and $H_2{}^{18}O$ (15 µl, 0.83 mmols) added. To this stirring solution $H_2{}^{18}O_2$ (300 µl, 3 x 10^{-3} mmols) was added and the solution injected directly into the mass spectrometer (CSI-MS -40ºC). The spectrum was collected immediately for 2 minutes. MS (CSI-MS) *m/z* 490.1 **(3Oc).**

[Fe^{III}(C$_8$H$_{14}$O$_2$)(^{Me,H}Pytacn)]$^+$ (4), {[Fe^{III}(C$_8$H$_{14}$(O)(OH))(^{Me,H}Pytacn)](CF$_3$SO$_3$)}$^+$ (5) (where **5** stands for **(4)+H$^+$+CF$_3$SO$_3$).**

[Fe(^{Me,H}Pytacn)(CF$_3$SO$_3$)$_2$] (**1**) (0.5 mg, 8 x 10^{-4} mmols) was dissolved in MeCN (~ 7 ml) and the solution cooled to 4 ºC. A solution of H_2O_2 (10 mM on 10 ml MeCN) was made up and also cooled to 4 ºC. The solution of **1** (300 µl) was added to a vial that was cooled in a dry ice/MeCN bath and

H_2O (15 µl, 0.83 mmols) added. To this stirring solution H_2O_2 (300 µl, 3 x 10^{-3} mmols) and cyclooctene (10 µl, 0.08 mmols) were added and the solution injected directly into the mass spectrometer (ESI-MS). The spectrum was collected for 2 mins. MS (ESI-MS) *m/z* 446.2 **(4)**, 596.2 **(5)**.

$[Fe^{III}(C_8H_{14}O(^{18}O))(^{Me,H}Pytacn)]^+$ (4a), $\{[Fe^{III}(C_8H_{14}(O)(^{18}OH))(^{Me,H}Pytacn)](CF_3SO_3)\}^+$ (5a) (where **5a** stands for **(4a)+H^++CF_3SO_3).**

[Fe(^{Me,H}Pytacn)(CF_3SO_3)$_2$] (**1**) (0.5 mg, 8 x 10^{-4} mmols) was dissolved in MeCN (~ 7 ml) and the solution cooled to 4 ºC. A solution of H_2O_2 (10 mM on 10 ml MeCN) was made up and also cooled to 4 ºC. The solution of **1** (300 µl) was added to a vial that was cooled in a dry ice/MeCN bath and $H_2{}^{18}O$ (15 µl, 0.83 mmols) added. To this stirring solution H_2O_2 (300 µl, 3 x 10^{-3} mmols) and cyclooctene (10 µl, 0.08 mmols) were added and the solution injected directly into the mass spectrometer (ESI-MS). The spectrum was collected for 2 mins. MS (ESI-MS) *m/z* 448.2 **(4a)**, 598.2 **(5a)**.

$[Fe^{III}(C_8H_{14}{}^{18}O(O))(^{Me,H}Pytacn)]^+$ (4b), $\{[Fe^{III}(C_8H_{14}(^{18}O)(OH))(^{Me,H}Pytacn)](CF_3SO_3)\}^+$ (5b) (where **5b** stands for **(4b)+H^++CF_3SO_3).**

[Fe(^{Me,H}Pytacn)(CF_3SO_3)$_2$] (**1**) (0.5 mg, 8 x 10^{-4} mmols) was dissolved in MeCN (~ 7 ml) and the solution cooled to 4 ºC. A solution of $H_2{}^{18}O_2$ (10 mM on 10 ml MeCN) was made up and also cooled to 4 ºC. The solution of **1** (300 µl) was added to a vial that was cooled in a dry ice/MeCN bath and H_2O (15 µl, 0.83 mmols) added. To this stirring solution $H_2{}^{18}O_2$ (300 µl, 3 x 10^{-3} mmols) and cyclooctene (10 µl, 0.08 mmols) were added and the solution injected directly into the mass spectrometer (ESI-MS). The spectrum was collected for 2 mins. MS (ESI-MS) *m/z* 448.2 **(4b)**, 598.2 **(5b).**

$[Fe^{III}(C_8H_{14}{}^{18}O(^{18}O))(^{Me,H}Pytacn)]^+$ (4c), $\{[Fe^{III}(C_8H_{14}(^{18}O)(^{18}OH))(^{Me,H}Pytacn)](CF_3SO_3)\}^+$ (5c) (where **5c** stands for **(4c)+H^++CF_3SO_3).**

[Fe(^{Me,H}Pytacn)(CF_3SO_3)$_2$] (**1**) (0.5 mg, 8 x 10^{-4} mmols) was dissolved in MeCN (~ 7 ml) and the solution cooled to 4 ºC. A solution of $H_2{}^{18}O_2$ (10 mM on 10 ml MeCN) was made up and also cooled to 4 ºC. The solution of **1** (300 µl) was added to a vial that was cooled in a dry ice/MeCN bath and $H_2{}^{18}O$ (15 µl, 0.83 mmols) added. To this stirring solution $H_2{}^{18}O_2$ (300 µl, 3 x 10^{-3} mmols) and cyclooctene (10 µl, 0.08 mmols) were added and the solution injected directly into the mass spectrometer (ESI-MS). The spectrum was collected for 2 mins. MS (ESI-MS) *m/z* 450.2 **(4c)**, 600.2 **(5c)**.

References

1 Ortiz de Montellano, P. R., *Cytochrome P450: Structure, Mechanism and Biochemistry*, 3erd ed. (Kluwer Academic/Plenum Publishers, New York, 2005).

2 Tshuva, E. Y. & Lippard S. J. Synthetic Models for Non-Heme Carboxylate-Bridged Diiron Metalloproteins: Strategies and Tactics *Chem. Rev.*, **104**, 987-1012 (2004).

3 Costas, M., Mehn, M. P., Jensen, M. P. & Que, L. Jr. Dioxygen Activation at Mononuclear Nonheme Iron Active Sites: Enzymes, Models, and Intermediates *Chem. Rev.*, **104**, 939-986 (2004).

4 Que, L. & Tolman, W. B. Biologically inspired oxidation catalysis *Nature*, **455**, 333-340 (2008).

5 Chen, M. S. & White M. C. A Predictable Selective Aliphatic C-H Oxidation Reaction for Complex Molecule Synthesis *Science*, **318**, 783-787 (2007).

6 Chen, M. S. & White, M. C. Combined Effects on Selectivity in Fe-Catalyzed Methylene Oxidation *Science*, **327**, 566-571 (2010).

7 Ferraro, D. J., Gakhar, L., & Ramaswamy, S. Rieske business: Structure–function of Rieske non-heme oxygenases *Biochem. Biophys. Res. Commun.*, **338**, 175-190 (2005).

8 Groves, J. T. High-valent iron in chemical and biological oxidations *J. Inorg. Biochem.*, **100**, 434-447 (2006).

9 Chakrabarty, S., Austin, R. N., Deng, D., Groves, J. T. & Lipscomb, J. D. Radical Intermediates in Monooxygenase Reactions of Rieske Dioxygenases *J. Am. Chem. Soc.* , **129**, 3514-3515 (2007).

10 Wolfe, M. D. et al. Benzoate 1,2-dioxygenase from Pseudomonas putida: Single Turnover Kinetics and Regulation of a Two-Component Rieske Dioxygenase *Biochemistry*, **41**, 9611-9626 (2002).

11 Rittle, J., Green, M. T. Cytochrome P450 Compound I: Capture, Characterization, and C-H Bond Activation Kinetics *Science,* **330**, 933-937 (2010).

12 Karlsson, A. et al. Crystal Structure of Naphthalene Dioxygenase: Side-on Binding of Dioxygen to Iron *Science*, **299**, 1039-1042 (2003).

13 Wolfe, M. D., Parales, J. V., Gibson, D. T. & Lipscomb, J. D. Single turnover chemistry and regulation of O_2 activation by the oxygenase component of naphthalene 1,2-dioxygenase *J. Biol. Chem.*, **276**, 1945-1953 (2001).

14 Gomez, L. et al. Stereospecific CH Oxidation with H_2O_2 Catalyzed by a Chemically Robust Site-Isolated Iron Catalyst *Angew. Chem. Int. Ed.*, **48**, 5720-5723 (2009).

15 Wolfe, M. D. & Lipscomb, J. D. Hydrogen Peroxide-coupled cis-diol Formation Catalyzed by Naphthalene 1,2-Dioxygenase *J. Biol. Chem.*, **278**, 829-835 (2003).

16 Chen, K. & Que, L. Jr. Stereospecific Alkane Hydroxylation by Nonheme Iron Catalysts: Mechanistic Evidence for an FeV=O Active Species *J. Am. Chem. Soc.*, **123**, 6327-6337 (2001).

17 Chen, K., Costas, M., Kim, J., Tipton, A. K. & Que, L. Jr. Olefin *cis*-Dihydroxylation versus Epoxidation by Nonheme Iron Catalysts: Two Faces of an Fe^{III}-OOH Coin *J. Am. Chem. Soc.*, **124**, 3026-3035 (2002).

18 Bassan, A., Blomberg, M. R. A., Siegbahn, P. E. M. & Que, L. Jr. Two Faces of a Biomimetic Non-Heme $HOFe^{V}O$ Oxidant: Olefin Epoxidation versus cis-Dihydroxylation *Angew. Chem. Int. Ed.*, **44**, 2939-2941 (2005).

19 Company, A. et al. Alkane Hydroxylation by a Nonheme Iron Catalyst that Challenges the Heme Paradigm for Oxygenase Action *J. Am. Chem. Soc.*, **129**, 15766-15767 (2007).

20 Company, A. et al. Olefin-Dependent Discrimination Between Two Nonheme $HO\text{-}Fe^{V}=O$ Tautomeric Species in Catalytic H_2O_2 Epoxidations *Chem. Eur. J.*, **15**, 3359-3362 (2009).

21 Yoon, J. et al., Reactive Intermediates in Oxygenation Reactions with Mononuclear Nonheme Iron Catalysts *Angew Chem. Int. Ed.* **48**, 1257-1260 (2009).

22 The first example of a non heme oxo-iron(V) species was spectroscopically characterized recently. This compound contains a tetraanionic kigand, which is likely to quench its electrophilicity, and it did not show C-H hydroxylation nor C=C cis-dihydroxylation reactivity. Oliveira, F. T. d. et al. Chemical and Spectroscopic Evidence for an Fe^{V}-Oxo Complex *Science*, **315**, 835-838 (2007).

23 A metastable S = 1/2 species assigned to Fe(V) was recently observed in catalytic epoxidation reactions by low-temperature reaction of non-heme iron complexes with peracids. Lyakin, O. Y., Bryliakov, K. P., Britovsek, G. J. P., & Talsi, E. P. EPR Spectroscopic Trapping of the Active Species of Nonheme Iron-Catalyzed Oxidation *J. Am. Chem. Soc.*, **131**, 10798–10799 (2009).

24 When this manuscript was under consideration, a non-heme catalyst that performs efficient cis-dihydroxylation of olefins with Oxone was reported. The authors describe MS characterization of a Fe(V) species. T. W. -S. Chow, E. L.-M. Wong, Z. Guo, Y. Liu, J. -S. Huang, C.-M. Che, *J. Am. Chem. Soc.*, **132**, 13229-13239 (2010)

25 Markert, C. & Pfaltz, A. Screening of Chiral Catalysts and Catalyst Mixtures by Mass Spectrometric Monitoring of Catalytic Intermediates *Angew. Chem. Int. Ed.*, **43**, 2498-2500 (2004).

26 Feichtinger, D. &. Plattner, D. A. Direct Proof for OMn^{v} (salen) Complexes *Angew. Chem. Int. Ed.*, **36**, 1718-1719 (1997).

27 Miras, H. N., Wilson, E. F. & Cronin, L. Unravelling the complexities of inorganic and supramolecular self-assembly in solution with electrospray and cryospray mass spectrometry *Chem. Commun.*, 1297-1311 (2009).

28 Wilson, E. F. et al. Probing the Self-Assembly of Inorganic Cluster Architectures in Solution with Cryospray Mass Spectrometry: Growth of Polyoxomolybdate Clusters and Polymers Mediated by Silver(I) Ions *J. Am. Chem. Soc.*, **130**, 13876-13884 (2008).

29 Yan, J., Long, D.-L., Wilson, E. F. & Cronin, L. Discovery of Heteroatom-Embedded Te{W18O54} Nanofunctional Polyoxometalates by Use of Cryospray Mass Spectrometry *Angew. Chem. Int. Ed.*, **48**, 4376-4380 (2009).

30 A time course experiment (Figure S3) shows that thermal decomposition of the $Fe^{V}(O)(OH)$ peak (M') results in formation of a novel undefined species with m/z = M'-2.

31 Ho, R. Y. N., Roelfes, G., Feringa, B. L. & Que, L., Jr. Raman Evidence for a Weakened O-O Bond in Mononuclear Low-Spin Iron(III)-Hydroperoxides *J. Am. Chem. Soc.*, **121**, 264-265 (1999).

32 Quinonero, D., Morokuma, K.; Musaev, D. G.; Mas-Balleste, R. & Que, L., Jr. Metal-Peroxo versus Metal-Oxo Oxidants in Non-Heme Iron-Catalyzed Olefin Oxidations: Computational and Experimental Studies on the Effect of Water *J. Am. Chem. Soc.*, **127**, 6548-6549 (2005).

33 Bassan, A. Blomberg, M. R. A. Siegbahn P. E. M. & Que, L. Jr. A Density Functional Study of O-O Bond Cleavage for a Biomimetic Non-Heme Iron Complex Demonstrating an Fe^{V}-Intermediate *J. Am. Chem. Soc.*, **124**, 11056-11063 (2002).

34 Ensing, B., Buda, F., Baerends, E. J. Fenton-like Chemistry in Water: Oxidation Catalysis by Fe(III) and H2O2, *J. Phys. Chem. A* **107**, 5722-5731 (2003).

35 DFT geometries were optimized at the B3LYP level in conjunction with the LANL2DZ basis set and associated ECP for Fe, and D95V basis set for the other atoms, as implemented in the Gaussian 09 program. The energies were further refined by single-point calculations with the SDD basis set and associated ECP for Fe, and the 6-311G(d,p) basis for the other atoms. Final free energies include energies computed at the B3LYP/SDD&6-311G(d,p)//B3LYP/LANLD2Z&D95V level of theory together with enthalpic and free energy corrections at the B3LYP/LANL2DZ&D95V level (See SI for further details and full reference).

36 a) P. Comba, G. Rajaraman, H. Rohwer, A Density Functional Theory Study of the Reaction of the Biomimetic Iron(II) Complex of a Tetradentate Bispidine Ligand with H2O2, *Inorg. Chem.* **46**, 3826-3838 (2007). b) Bukowski, M. R. et al., Catalytic epoxidation and 1,2-dihydroxylation of olefins with bispidine-iron(II)/H2O2 systems *Angew. Chem. Int. Ed.* **45**, 3446-3449 (2006).

37 Oldenburg, P. D., Feng, Y., Pryjomska-Ray, I., Ness, D., Que, L. Jr., Olefin Cis-Dihydroxylation with Bio-Inspired Iron Catalysts. Evidence for an FeII/FeIV Catalytic Cycle *J. Am. Chem. Soc.* **132**, 17713 (2010).

38 Company, A. et al., Modelling the cis-oxo-labile binding site motif of non-heme iron oxygenases. Water exchange and remarkable oxidation reactivity of a novel non-heme iron(IV)-oxo compound bearing a tripodal tetradentate ligand, *Chem. Eur. J.* **17**, 1622-1634 (2010).

Acknowledgements

We would like to thank the EPSRC, WestCHEM for funding and Bruker Daltonics for collaboration. LC thanks the Royal Society / Wolfson foundation for a merit award. MC thanks MICINN for project CTQ2009-08464, Generalitat de Catalunya for an ICREA Academia Award and the European Research Foundation for Project ERC-2009-StG-239910

Author Contributions

LC and MC devised the initial concept for the work and LC, MC, XR, JSM, IP, JML, MG designed the experiments and JSM, MG and IP carried out the experiments and analysed the data. MC and LC wrote the manuscript.

Competing Interests Statement: The authors have no competing interests.